Spatio-Spectral Analysis on the Sphere Using Spatially Localized Spherical Harmonics Transform

Zubair Khalid, Salman Durrani, Parastoo Sadeghi, and
Rodney A. Kennedy

Abstract—This correspondence studies a spatially localized spectral transform for signals on the unit sphere, which we call spatially localized spherical harmonics transform (SLSHT). For a systematic treatment, we explicitly express the transform in terms of rotated versions of an azimuthally symmetric window function and introduce the spatio-spectral SLSHT distribution with a succinct matrix representation. We present guidelines for the choice of the window function in the SLSHT, based on the inherent tradeoff between the spatial and spectral resolution of different window functions from the perspective of the uncertainty principle. We demonstrate the use of an eigenfunction window, obtained from the Slepian concentration problem on the sphere, as a good choice for window function. As an illustration, we apply the transform to the topographic map of Mars, which can reveal spatially localized spectral contributions that were not obtainable from traditional spherical harmonics analysis.

Index Terms—Signal analysis, spectral analysis, spheres, spherical harmonics.

I. INTRODUCTION

Development of spatio-spectral analysis techniques for signals defined on the unit sphere is of interest in various fields of science and engineering, such as analysis of planetary gravity and topography data in geophysics [1]–[3]. While any signal on the sphere can be expressed in terms of spherical harmonics, these functions are not spatially concentrated and therefore not well suited for joint spatio-spectral analysis. For such analysis, most of the existing methods available in the literature are based on spherical wavelets [3]–[9], which enable space-scale decomposition of a signal on the sphere. With a suitable choice of a mother wavelet, some of these wavelet based techniques can also discriminate directional phenomena [3]–[6].

An alternative to the wavelet (i.e., space-scale) approach is a "space-spectral" approach, where the goal is to obtain a joint spatio-spectral distribution of signals defined on the sphere as an analog of the widely used short-time Fourier transform (STFT) in time-frequency analysis [10], [11]. Such a space-spectral decomposition reveals the localized contribution of spherical harmonics in the global signal. It should be noted that space-spectral and space-scale approaches are complementary, with the most appropriate choice depending on the properties of the signal under analysis. In general, the finite support on the sphere makes it non-trivial to emulate and extend familiar operations in Euclidean domain to the spherical domain. A localized spectral analysis using windowing operation has been studied in [1], which investigates the spatio-spectral relationships between two

signals on the sphere. Spectral estimation techniques using multiple window functions obtained from Slepian's concentration problem on the sphere have been proposed in [12] and [13]. A spatio-spectral localization method based on spatial windowing followed by spectral decomposition is proposed in [2]. The method has an advantage of being in the spirit of conventional time-frequency analysis techniques which use windowing. It is shown that the localized transform is invertible by spatial averaging of the transform. The effectiveness of the transform, however, depends on the chosen window function. The authors in [2] use a window function which is spectrally concentrated, but exhibits sidelobes in the spatial domain. Also no guidelines are presented for the choice of window function.

In this correspondence, we present a matrix formulation of the transform in [2], which we call spatially localized spherical harmonics transform (SLSHT) as an analog of the STFT in time-frequency analysis. For this purpose, we focus on the use of azimuthally symmetric window functions (centered at the north pole) to achieve localization in the spatial domain and express the transform in terms of the rotation applied to the original window. We also give a succinct matrix representation of all possible SLSHT components, which we refer to as SLSHT distribution. We discuss the inherent tradeoff between the spatial and spectral resolution of different window functions from the perspective of the uncertainty principle. We propose and demonstrate the use of an eigenfunction window, obtained from the Slepian concentration problem on sphere [12], as a good choice for window function in the SLSHT. As an illustration, we apply the SLSHT distribution with eigenfunction window to the example of the Mars topographic map and show that the localized contributions of spherical harmonics are apparent in the spatio-spectral domain. The rest of the correspondence is organized as follows. In Section II, we present the system model. The matrix formulation of the SLSHT and signal inversion is presented in Section III. The window localization tradeoff is discussed in Section IV. Results are presented in Section V. Finally, concluding remarks are given in Section VI.

The following notation and terms are used in this paper: lowercase bold symbols correspond to vectors whereas uppercase bold symbols denote matrices. $\overline{(\cdot)}$ denotes the complex conjugate operation and $|(\cdot)|$ denotes the magnitude. δ denotes the Kronecker delta function defined as $\delta_{ab} = 1$ if $a = b$ and $\delta_{ab} = 0$ if $a \neq b$.

II. MATHEMATICAL BACKGROUND

Let $f(\theta, \phi)$ be a complex valued function, defined on the unit sphere $\mathbb{S}^2 \triangleq \{\mathbf{r} \in \mathbb{R}^3 : \|\mathbf{r}\| = 1\}$, that is, if $\mathbf{r} \in \mathbb{S}^2$ then $\mathbf{r}$ is a unit vector, $\theta \in [0, \pi]$ denotes colatitude measured with respect to the positive z-axis and $\phi \in [0, 2\pi)$ denotes longitude measured with respect to the positive x-axis in the $x - y$ plane. Let f and g be two functions on the unit sphere and define the inner product

$$\langle f, g \rangle \triangleq \int_{\mathbb{S}^2} f(\Omega)\overline{g(\Omega)}d\Omega \tag{1}$$

where $\Omega \equiv \{\theta, \phi\}$ parameterizes a point on the unit sphere and $d\Omega = \sin\theta d\theta d\phi$. Finite energy functions whose domain is the unit sphere are referred to as "signals on the unit sphere" or simply "signal". Mathematically, f is a signal on the unit sphere if and only if it has finite induced norm $\|f\| \triangleq \langle f, f \rangle^{\frac{1}{2}} < \infty$. All such finite energy signals under inner product (1) form a complex Hilbert space $L^2(\mathbb{S}^2)$.

The spherical harmonics $Y_\ell^m(\theta, \phi)$ [14] form an orthonormal set of basis functions on the sphere with respect to the inner product in (1). By completeness, any signal $f \in L^2(\mathbb{S}^2)$ can be expanded as

$$f(\theta, \phi) = \sum_{\ell=0}^{\infty} \sum_{m=-\ell}^{\ell} f_\ell^m Y_\ell^m(\theta, \phi) \tag{2}$$

where f_ℓ^m are the spherical harmonic Fourier coefficients of degree ℓ and order m, given by

$$f_\ell^m = \langle f, Y_\ell^m \rangle = \int_{\mathbb{S}^2} f(\theta, \phi) \overline{Y_\ell^m(\theta, \phi)} d\Omega. \tag{3}$$

In this work, we express spherical harmonics Y_ℓ^m as Y_c (and f_ℓ^m as f_c), that is, as a function of a single integer index c instead of two integer indices ℓ and m, using the one-to-one mapping $(\ell, m) \leftrightarrow c$, where $c = \ell^2 + \ell + m$. With this notation, the two summations in (2) can be written as one summation and a product of functions in the spherical harmonic domain can be expressed more succinctly.

A proper rotation of a signal on the sphere can be parameterized in terms of the Euler angles, $\alpha \in [0, 2\pi)$, $\beta \in [0, \pi]$, $\gamma \in [0, 2\pi)$. Define the rotation operator $D(\alpha, \beta, \gamma)$ which rotates a signal first as a γ rotation about z-axis, followed by a β rotation about y-axis, and then an α rotation about z-axis. If a signal $f(\theta, \phi)$ is rotated on the sphere under rotation operator $D(\alpha, \beta, \gamma)$, each spherical harmonic coefficient f_ℓ^m of degree ℓ and order m is transformed into a linear combination of different order spherical harmonics of the *same* degree ℓ as

$$\left\{ D(\alpha, \beta, \gamma) f \right\}_\ell^m = \left\langle D(\alpha, \beta, \gamma) f, Y_\ell^m \right\rangle = \sum_{m'=-\ell}^{\ell} D_\ell^{m,m'}(\alpha, \beta, \gamma) f_\ell^{m'} \tag{4}$$

where $D_\ell^{m,m'}(\alpha, \beta, \gamma)$ is the Wigner-D function [14].

For azimuthally symmetric signals which are invariant of γ, the operator $D(\alpha, \beta, \gamma)$ simplifies to the special type of rotation operator $D_\Omega \triangleq D(\phi, \theta, 0)$ which has the effect of rotating a signal first through an angle of θ about the y-axis followed by an angle of ϕ about the z-axis. Similarly, given (4), the only relevant Wigner-D function when operating on azimuthally symmetric signals, occurs when $m' = 0$ and in this case it can be expressed in terms of spherical harmonics as [15]

$$D_\ell^{m,0}(\phi, \theta, 0) = \sqrt{\frac{4\pi}{2\ell+1}} \overline{Y_\ell^m(\theta, \phi)}. \tag{5}$$

III. FORMULATION OF SLSHT

In this section, we present a matrix formulation of SLSHT to transform a signal to joint spatio-spectral domain. We first define the SLSHT and use it to define the SLSHT distribution.

Definition 1 (Spatially Localized Spherical Harmonics Transform): The SLSHT of signal $f \in L^2(\mathbb{S}^2)$ is given by

$$g(\Omega, c) \triangleq \int_{\mathbb{S}^2} f(\Omega') \left(D_\Omega h \right)(\Omega') \overline{Y_c(\Omega')} d\Omega' \tag{6}$$

where $h \in L^2(\mathbb{S}^2)$ is an azimuthally symmetric window such that $\langle h, Y_\ell^m \rangle = 0$ for all $m \neq 0$ and $D_\Omega \triangleq D(\phi, \theta, 0)$ is the simplified rotation operator.

Remark 1: The SLSHT represents the contribution of the spherical harmonic Y_c of index c (degree ℓ and order m) within a symmetric spatial domain centered on Ω for the signal f. Note that the relocation, through rotation, of the window function in (6) is not explicitly defined in [2].

Definition 2 (Spatially Localized Spherical Harmonics Transform Distribution): The SLSHT distribution $\mathbf{g}$ of a signal $f \in L^2(\mathbb{S}^2)$ is an indexed vector of all SLSHT components of the form $g(\Omega, c)$ as defined in (6) for $c = 0, 1, \ldots, C$, i.e.,

$$\mathbf{g}(\Omega) = \left[g(\Omega, 0), g(\Omega, 1), g(\Omega, 2), \ldots, g(\Omega, C) \right] \tag{7}$$

where $C = L^2 + 2L$, $L = L_f + L_h$, and L_f and L_h denote the maximum spectral degree of the signal f and azimuthally symmetric window function h, respectively.

Remark 2: The SLSHT distribution is a generalization of the transform in [2] and provides the complete spatio-spectral representation of a signal.

Remark 3: It is implicit in the formulation of SLSHT that the signal of interest is bandlimited to $L_f < \infty$. As a signal is finite energy, then its spherical harmonic Fourier coefficients are square summable. Consequently, any signal can be arbitrarily closely approximated by a bandlimited signal by making L_f sufficiently large. The study of the involved approximation errors on the SLSHT is outside the scope of this correspondence.

A. Matrix Representation

First we determine the spherical harmonic coefficients corresponding to the rotated window as

$$\begin{aligned} w_b(\Omega) &\triangleq \langle D_\Omega h, Y_b \rangle \\ &= D_p^{q,0}(\phi, \theta, 0) h_p^0, \quad (p, q) \leftrightarrow b, \ \Omega \equiv \{\theta, \phi\} \\ &= \sqrt{\frac{4\pi}{2p+1}} \overline{Y_b(\Omega)} h_p^0, \quad (p, q) \leftrightarrow b. \end{aligned} \tag{8}$$

Using the mapping $(\ell, m) \leftrightarrow c$, $(\ell', m') \leftrightarrow a$ and $(p, q) \leftrightarrow b$, we write $g(\Omega, c)$ in (6) as

$$g(\Omega, c) = \sum_{a=0}^{A} f_a \sum_{b=0}^{B} w_b(\Omega) y(a, b, c) \tag{9}$$

where $f_a = \langle f, Y_a \rangle$, $A = (L_f)^2 + 2L_f$, $B = (L_h)^2 + 2L_h$ and

$$y(a, b, c) \triangleq \int_{\mathbb{S}^2} Y_a(\Omega) Y_b(\Omega) \overline{Y_c(\Omega)} d\Omega \tag{10}$$

denotes the spherical harmonics triple product and can be calculated using Wigner-$3j$ functions [1]. From (9), we can express the SLSHT distribution as

$$\mathbf{g}(\Omega) = \mathbf{f} \mathbf{\Psi}(\Omega) \tag{11}$$

where $\mathbf{f} = \left[f_0, f_1, f_2, \ldots, f_A \right]$ is the spectral response of bandlimited signal f with bandwidth L_f (and $A = (L_f)^2 + 2L_f$), and $\mathbf{\Psi}(\Omega)$ is the transformation matrix of size $(A+1) \times (C+1)$ given by

$$\mathbf{\Psi}(\Omega) = \begin{bmatrix} \psi_{00} & \psi_{01} & \cdots & \psi_{0C} \\ \psi_{10} & \psi_{11} & \cdots & \psi_{1C} \\ \vdots & \vdots & & \vdots \\ \psi_{A0} & \psi_{A1} & \cdots & \psi_{AC} \end{bmatrix} \tag{12}$$

with entries

$$\psi_{ac} \equiv \psi_{ac}(\Omega) = \sum_{b=0}^{B} w_b(\Omega) y(a, b, c). \tag{13}$$

Remark 4: The matrix form in (11) projects the spectral response of the signal $\mathbf{f}$ to the joint spatio-spectral domain. The size of the transformation matrix is dependent on the spectral bandwidth of the input signal f and the window function h. The value of matrix elements is dependent on the applied rotation Ω and the window function h, whose choice will be discussed in Section IV.
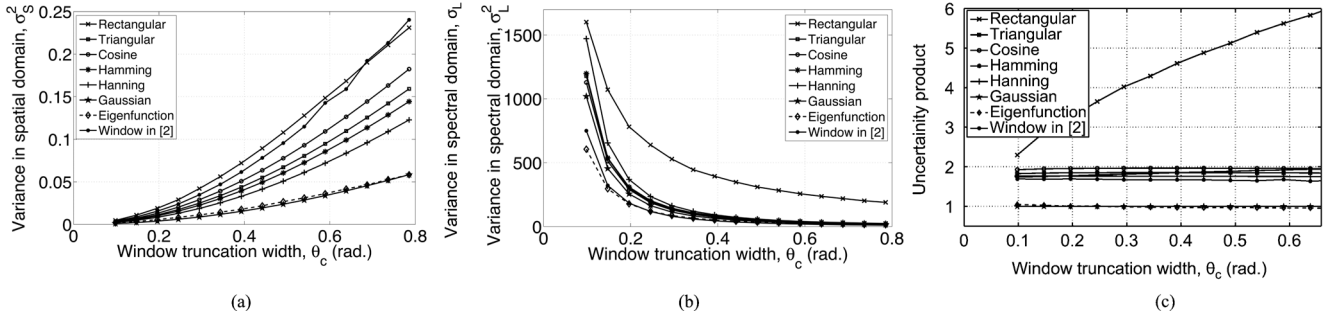
Fig. 1. (a) Variance σ_{S}^2 in spatial domain (b) variance σ_{L}^2 in spectral domain and (c) uncertainty product in (19) for different types of azimuthally symmetric window functions.

B. Inversion as Spherical Harmonics Marginal

Recovery of the spectral components of the signal from its localized transform was first shown in [2]. For the sake of completeness, based on our matrix formulation, and explicit expression of the transform in terms of rotated window function, we provide an alternative formulation.

Theorem 1 (Inversion of Signal From SLSHT Distribution): If $\mathbf{g}(\Omega)$ represents the SLSHT distribution of the signal f using azimuthally symmetric window function h, where the distribution is of the form (7), then the spectral domain response $\mathbf{f}$ of f can be recovered from $\mathbf{g}(\Omega)$ up to a multiplicative factor as the spherical harmonics marginal $\hat{\mathbf{f}}$, which is obtained by integrating the SLSHT distribution over the spatial domain as

$$\hat{\mathbf{f}} = \int_{\mathbb{S}^2} \mathbf{g}(\Omega) d\Omega = \sqrt{4\pi}\, h_0^0 \times \left[f_0, f_1, \ldots, f_A, 0, \ldots, 0 \right] \quad (14)$$

where $\hat{\mathbf{f}}$ denotes the spherical harmonics marginal and is a row vector of length $C + 1$ where only the first $A + 1$ elements are nonzero.

Proof: Integrating (7) over the spatial domain gives

$$\int_{\mathbb{S}^2} \mathbf{g}(\Omega) d\Omega = \mathbf{f} \int_{\mathbb{S}^2} \mathbf{\Psi}(\Omega) d\Omega. \quad (15)$$

The integral of kernel matrix $\mathbf{\Psi}$ is obtained by integrating each matrix element $\psi_{ac}(\Omega)$ in (13), i.e.,

$$\int_{\mathbb{S}^2} \psi_{ac}(\Omega) d\Omega = \sum_{b=0}^{B} y(a, b, c) \int_{\mathbb{S}^2} w_b(\Omega) d\Omega. \quad (16)$$

Now, using the definition of w_b in (8) with mapping $(p, q) \leftrightarrow b$ and the result from (5), we obtain

$$\int_{\mathbb{S}^2} w_b(\Omega) d\Omega = \int_{\mathbb{S}^2} \sqrt{\frac{4\pi}{2p+1}}\, \overline{Y_p^q(\theta, \phi)} h_p^0 d\Omega = 4\pi h_0^0 \delta_{p0}\delta_{q0} = 4\pi h_0^0 \delta_{b0}. \quad (17)$$

Using (17), all the summation terms in (16) become zero except for $b = 0$. From the orthonormal property of spherical harmonics, $y(a, 0, c) = \frac{\delta_{ac}}{\sqrt{4\pi}}$. Incorporating these results in (16), we get

$$\int_{\mathbb{S}^2} \psi_{ac}(\Omega) d\Omega = \sqrt{4\pi} h_0^0 \delta_{ac}. \quad (18)$$

Substituting (18) in integrating the elements of $\mathbf{\Psi}(\Omega)$ in (15), we obtain (14). ∎

Remark 5: From the result in Theorem 1, we can see that we only need to know the DC component of the window function in order to recover the signal exactly from its SLSHT distribution.

IV. OPTIMAL SPATIO-SPECTRAL CONCENTRATION OF WINDOW FUNCTION

The SLSHT distribution does not depend solely on the signal because the distribution entangles the signal and the window. The effectiveness of SLSHT distribution depends on the chosen window function. If we require a higher resolution in one domain, the window should be narrower in that domain. From the uncertainty principle on the unit sphere, a signal cannot be locally concentrated in both the spatial and spectral domains [9]. If a window is chosen to obtain the desired resolution in one domain, it is said to be an optimal window if it is also optimally localized in the other domain [10].

We study the window functions jointly in both spatial and spectral domains using the definition of uncertainty principle on the unit sphere. The following inequality, referred as uncertainty principle, holds for unit energy azimuthally symmetric functions defined on the unit sphere [9], [16]

$$\frac{\sigma_{\mathrm{S}}}{\sqrt{1 - \sigma_{\mathrm{S}}^2}} \cdot \sigma_{\mathrm{L}} \geq 1 \quad (19)$$

where σ_{S}^2 and σ_{L}^2 denote the variance of the window function in the spatial domain and spectral domain respectively and are defined as [1], [9]

$$\sigma_{\mathrm{S}}^2 = 1 - \left(\pi \int_0^\pi \sin(2\theta) \left| h(\theta) \right|^2 d\theta \right)^2,$$

$$\sigma_{\mathrm{L}}^2 = \sum_{\ell=0}^\infty \ell(\ell+1) |h_\ell^0|^2. \quad (20)$$

Note that a unit energy window function is assumed in (20), which ensures that $0 \leq \sigma_{\mathrm{S}} \leq 1$.

In this work, we consider and compare the following unit energy normalized azimuthally symmetric window functions: rectangular window, triangular window, cosine window, Hamming window, Hanning window, the window of Simons *et al.* [2], Gaussian window and the *eigenfunction window*, all of which are parameterized by θ_c denoting the window truncation width. The first five windows are defined in [17]. The window in [2] is obtained by truncating the rectangular window in the spectral domain within the main spectral lobe. The Gaussian window is a unit energy normalized function that decays exponentially with the square of the colatitude and its variance is chosen such that 99% of the energy lies within the truncation width [18]. The eigenfunction window $h(\Omega)$ arises as a solution of Slepian concentration problem on the sphere [19]. To maximize the spatial concentration of a bandlimited signal $h(\Omega)$ with maximum spherical harmonic degree L_h, equivalently represented by the column vector $\mathbf{h}$ containing the entries h_ℓ^0 for $0 \leq \ell \leq L_h$, within a polar cap
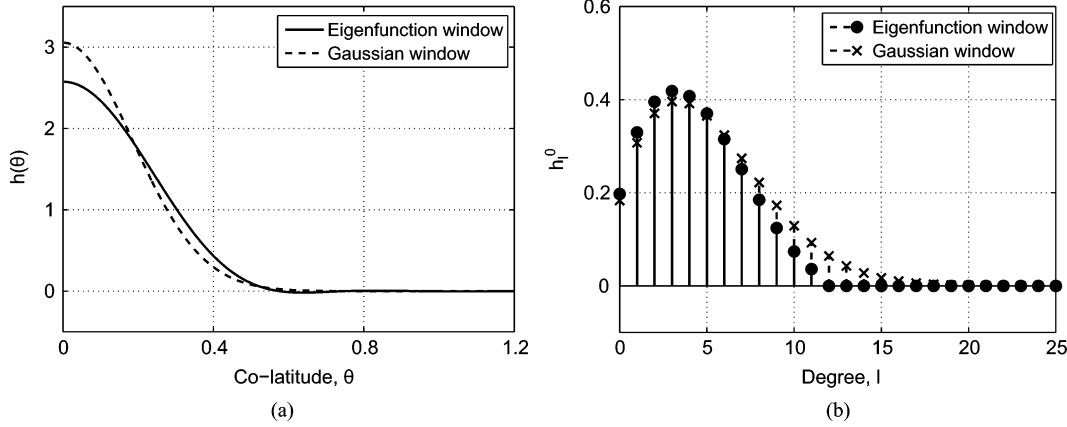
Fig. 2. Gaussian window and eigenfunction window for truncation width, $\theta_c = \frac{\pi}{6}$ in (a) spatial domain, $h(\Omega) = h(\theta)$ and (b) spectral domain, h_ℓ^0. Eigenfunction window has less spectral bandwidth relative to the Gaussian window.
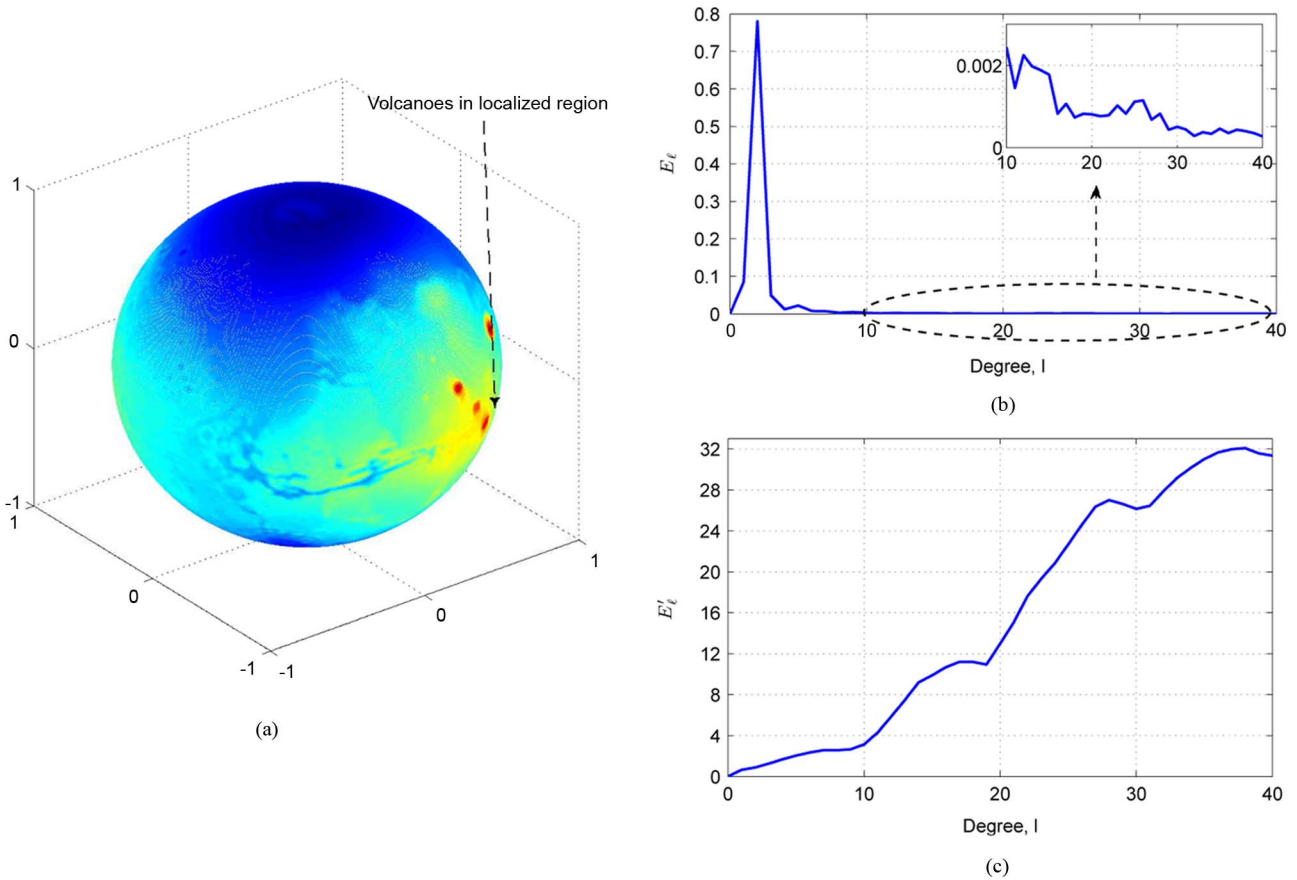

Fig. 3. (a) Mars topographic map $f(\Omega)$, obtained using bandlimited spectral model of Mars with maximum spectral degree 150. (b) Energy per spherical harmonic degree E_ℓ (22). (c) Energy ratio per degree E'_ℓ in (23) for components of SLSHT distribution $\mathbf{g}$ in (7) of Mars topographic map for degree $0 \leq \ell \leq 40$.

region R characterized by truncation width θ_c, one needs to maximize the spatial concentration ratio [1], [19]

$$\lambda = \frac{\int_R |h(\Omega)|^2 d\Omega}{\int_{\mathbb{S}^2} |h(\Omega)|^2 d\Omega}. \qquad (21)$$

The solution that maximizes (21) gives rise to the standard eigenvalue problem $\mathbf{D}\mathbf{h} = \lambda \mathbf{h}$, which can be solved numerically. As we are considering azimuthally symmetric region R, $\mathbf{h} = [h_0^0, h_1^0, \ldots, h_{L_h}^0]$ denotes the spectral response of $h(\Omega)$ and $\mathbf{D}$ is the $(L_h + 1) \times (L_h + 1)$ real and symmetric matrix where the entries

are given by $D_{\ell\ell'} = \int_R Y_\ell^0(\Omega) Y_{\ell'}^0(\Omega) d\Omega$. We use the band-limited eigenfunction as window function, the one with the largest eigenvalue and minimum possible bandwidth L_h related to truncation width θ_c as $L_h = \left(\frac{2\pi}{\theta_c}\right) - 1$ [19].

Fig. 1 plots the (a) variance σ_S^2 in spatial domain, (b) variance σ_L^2 in spectral domain and (c) uncertainty product in (19) for different types of azimuthally symmetric window functions and different values of truncation width $\frac{\pi}{32} \leq \theta_c \leq \frac{\pi}{4}$. Fig. 1(a) and (b) shows that generally the variance in spatial domain increases with the truncation width and the variance in spectral domain decreases with the truncation width.
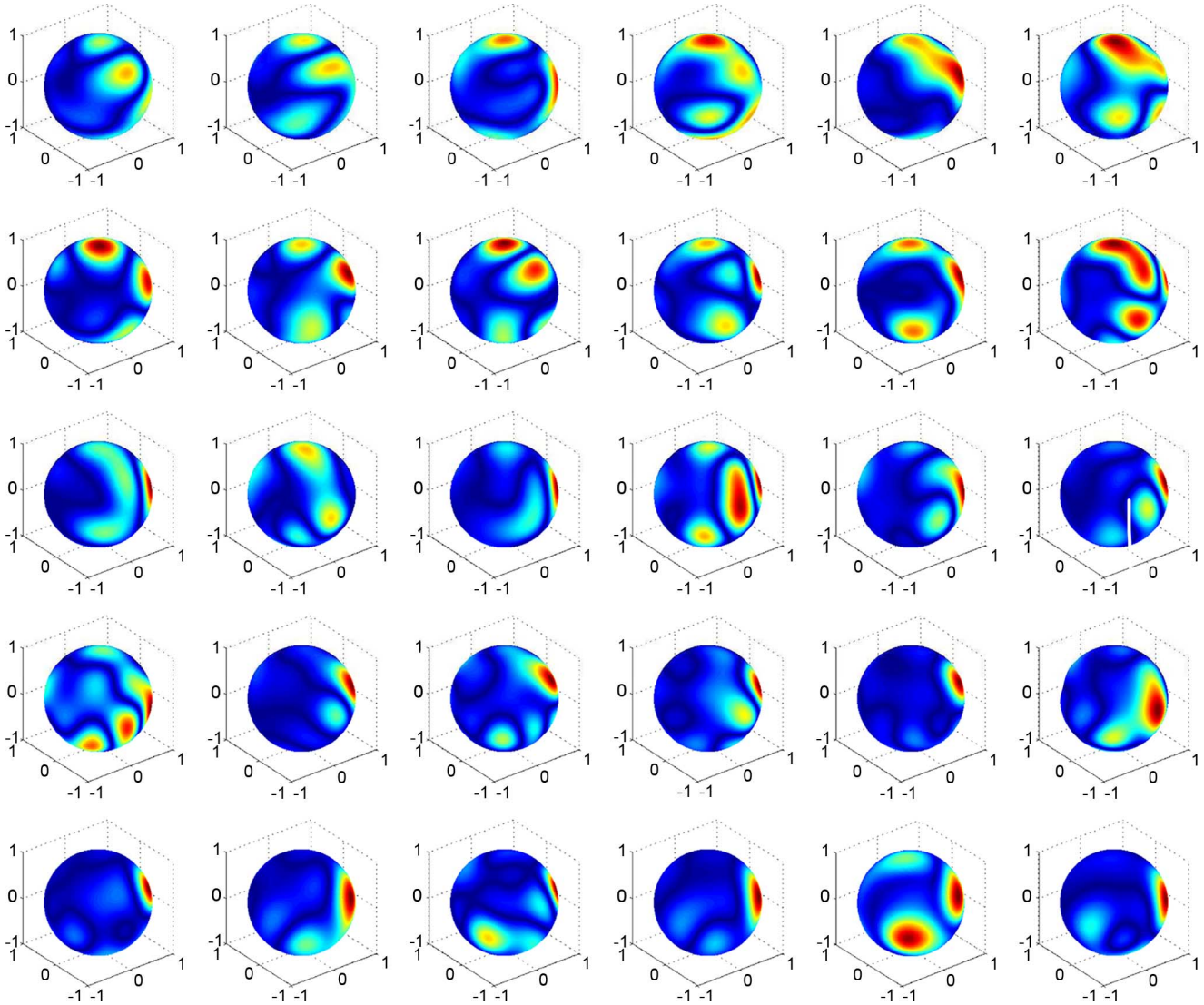
Fig. 4. Magnitude of components of SLSHT distribution **g** in (7) of Mars topographic map $f(\Omega)$. The distribution components $g(\Omega, \ell, m)$ are shown for $m = 0$ and $11 \le \ell \le 40$ in a sorted manner; that the degree ℓ increments from left to right, with the lowest degree $\ell = 11$ is plotted on the top left and the highest degree $\ell = 40$ on the lower right. Blue indicates low magnitude while red indicates high magnitude.

The rectangular window has the poorest localization because the discontinuity at truncation points increases its variance in the spectral domain. As expected, the window in [2] performs very well in the spectral domain, but poorly in the spatial domain. The figure also shows that the Gaussian window and the eigenfunction window exhibit better localization behavior. Comparatively, these two windows have the lowest variances in both domains. Note that the smaller value for variance indicates better localization. Fig. 1(c) confirms that both the eigenfunction window and the Gaussian window nearly attain the lower bound of 1 for the uncertainty product of (19). The rectangular window has the largest uncertainty product as expected. The product for other windows, including the window in [2], lie between these two extremes.

The optimal truncation width depends on the required resolution in both the spatial and spectral domains. As indicated in the variance plot in Fig. 1, the spatial variance σ_S^2 of eigenfunction window is very close to that of Gaussian window. But the spectral variance σ_L^2 of eigenfunction window is lower than that of Gaussian window, especially at lower truncation widths. The Gaussian window and eigenfunction window are plotted for truncation width $\theta_c = \frac{\pi}{6}$ in both spatial and spectral domains in Fig. 2. Both windows are normalized to unit energy and

chosen such that 99% of energy lies within the truncation width. It is observed that the eigenfunction window has smaller bandwidth and its energy is more uniformly distributed relative to Gaussian window. Thus, the eigenfunction window can be a good choice for window function in the SLSHT distribution.

It must be noted that compared to space-scale techniques, the space-spectral resolution of the SLSHT is fixed for all spectral components and spatial positions. Incorporating multi-resolution capability in SLSHT is possible, but would require using different bandwidth window functions for different SLSHT distribution components, consideration of which is beyond the scope of this correspondence. Finally, we remark that with appropriate modifications it is possible to incorporate non-azimuthally symmetric windows into our formulation.

V. SIMULATION RESULTS

In this section, we demonstrate the spatially localized spherical harmonics transform and our proposed window to study the signals in joint spatio-spectral domain. We consider a Mars signal on the sphere that has higher degree harmonic components in a localized mountainous spatial region. We study the high resolution Mars topographic map

(size = 800×800) using SLSHT and illustrate that the SLSHT distribution reveals localized spectral contributions of spherical harmonics in the spatial domain. In the simulation results, we have implemented the method outlined in [15] to calculate the spherical harmonic components and triple product in Matlab. We use equiangular sampling with $N \times N$ samples on the sphere as $\theta_n = \frac{\pi n}{N}$, $\phi_n = \frac{2\pi n}{N}$ for $n = 0, 1, \ldots, N-1$. Note that exact quadrature can be performed using this tessellation with errors on the order of numerical precision. We use the azimuthally symmetric bandlimited Slepian eigenfunction window to obtain the localization in spatial domain. For SLSHT distribution computation using a window with bandwidth L_h, we use a very high resolution $N = 800 \gg 2L_h$ to obtain smooth plots. Finally, for inverse spherical harmonic transform of a function with maximum spherical harmonics degree L_f, we use minimum resolution $N = 2L_f + 1$ [15] for exact quadrature.

Fig. 3(a) shows the Mars topographic map $f(\Omega)$ in the spatial domain. The Mars topographic map $f(\Omega)$ is obtained in the spatial domain using its spherical harmonics topographic model up to degree of 150. There are volcanoes leading to high frequency contents in the signal which are localized in the vicinity of $\theta = \frac{\pi}{2}$ and $\phi = \frac{-\pi}{3}$. We use the unit energy normalized Mars signal with DC-component eliminated. If f_ℓ^m denotes the spherical harmonic coefficients for the Mars signal $f(\Omega)$, we define the energy per degree E_ℓ as

$$E_\ell = \sum_{m=-\ell}^{\ell} |f_\ell^m|^2. \tag{22}$$

Fig. 3(b) shows the energy per degree E_ℓ in the spectrum of Mars, which indicates that 90% of the energy is contributed by the spherical harmonics with degree less than 10. The higher degree spherical harmonics contribute towards high frequency regions in a signal and contain very little amount of energy. The higher degree spherical harmonic coefficients do not reveal information about the region of their contributions in the signal $f(\Omega)$. We determine all SLSHT components of the form $g(\Omega, c)$ for $1 \le c \le 1671$ or $g(\Omega, \ell, m)$ for $1 \le \ell \le 40$ and all orders $|m| \le \ell$ using an eigenfunction window with truncation width $\theta_c = \frac{\pi}{8}$. We calculate the energy contribution by spherical harmonics in a region around volcanoes. We expect that higher spherical harmonics would have significant energy concentrated around the volcanoes region. We define the energy ratio per degree E'_ℓ as a measure of energy contribution by all order spherical harmonics for a particular degree in the localized region as

$$E'_\ell = \sum_{m=-\ell}^{\ell} \frac{\int_R |g(\Omega, \ell, m)|^2 d\Omega}{\int_{\mathbb{S}^2} |g(\Omega, \ell, m)|^2 d\Omega} \tag{23}$$

where R denotes the spherical cap region of width $\frac{\pi}{8}$ centered at $\theta = \frac{\pi}{2}$ and $\phi = \frac{-\pi}{3}$. The region R only covers 3.81% area of the whole sphere and captures the magnitude of SLSHT distribution component around the volcanoes region. Fig. 3(c) shows the energy ratio per degree E'_ℓ, which indicates that the higher degree spherical harmonics, despite of their low energy content in overall spectrum, have their energy localized in a region R.

Fig. 4 shows the magnitude of zero order distribution components of the form $g(\Omega, \ell, 0)$ for $11 \le \ell \le 40$, which indicate the spatial contribution of zero order spherical harmonics. These distribution components indicate that the contribution of higher order spherical harmonics is mainly around the region where volcanoes are located. Note that it is also possible to resolve topographic features such as volcanoes using wavelets, as demonstrated in [3]. However, the SLSHT distribution provides interpretation about the spectral contributions of a particular spherical harmonic in a localized region in the spatial domain, which is not explicitly possible using wavelets and for the case of Mars, also not clearly visible in the global spectrum of the signal.

VI. CONCLUSION

In this correspondence, we have studied the spatially localized spherical harmonics transform (SLSHT), for transforming signals on the sphere into joint spatio-spectral SLSHT distribution that represents how the signal spectrum is changing in spatial domain. We formulated the matrix representation of the transform. We used an azimuthally symmetric window function to achieve spatial localization and analyzed the localization tradeoff for different window functions in both spatial and spectral domains from the perspective of the uncertainty principle. As an illustration, we analyzed the topographic map of Mars and demonstrated that the SLSHT distribution reveals the spatially localized contributions of spherical harmonics, which cannot be obtained from the global signal spectrum. The knowledge of the spatially localized contributions of spherical harmonics obtained via SLSHT can be used to develop techniques for filtering and processing of signals on the sphere in the joint spatio-spectral domain.

REFERENCES

[1] M. Wieczorek and F. J. Simons, "Localized spectral analysis on the sphere," *Geophys. J. Int.*, vol. 131, no. 1, pp. 655–675, May 2005.

[2] M. Simons, S. C. Solomon, and B. H. Hager, "Localization of gravity and topography: Constraints on the tectonics and mantle dynamics of Venus," *Geophys. J. Int.*, vol. 131, no. 1, pp. 24–44, Oct. 1997.

[3] P. Audet, "Directional wavelet analysis on the sphere: Application to gravity and topography of the terrestrial planets," *J. Geophys. Res.*, vol. 116, Feb. 2011 [Online]. Available: http://www.agu.org/pubs/crossref/2011/2010JE003710.shtml

[4] Y. Wiaux, J. D. McEwen, P. Vandergheynst, and O. Blanc, "Exact reconstruction with directional wavelets on the sphere," *Mon. Not. R. Astron. Soc.*, vol. 388, no. 2, pp. 770–788, 2008.

[5] J. D. McEwen, M. P. Hobson, D. J. Mortlock, and A. N. Lasenby, "Fast directional continuous spherical wavelet transform algorithms," *IEEE Trans. Signal Process.*, vol. 55, no. 2, pp. 520–529, Feb. 2007.

[6] J. D. McEwen, M. P. Hobson, and A. N. Lasenby, "A directional continuous wavelet transform on the sphere," *ArXiv preprint astro-ph/0609159*, 2006 [Online]. Available: http://arxiv.org/abs/astro-ph/0609159

[7] J.-L. Starck, Y. Moudden, P. Abrial, and M. Nguyen, "Wavelets, ridgelets and curvelets on the sphere," *Astron. Astrophys.*, vol. 446, pp. 1191–1204, Feb. 2006.

[8] J.-P. Antoine and P. Vandergheynst, "Wavelets on the 2-sphere: A group-theoretical approach," *Appl. Comput. Harmon. Anal.*, vol. 7, pp. 262–291, 1999.

[9] F. J. Narcowich and J. D. Ward, "Non-stationary wavelets on the m-sphere for scattered data," *Appl. Comput. Harmon. Anal.*, vol. 3, no. 4, pp. 324–336, Oct. 1996.

[10] L. Cohen, "Time-frequency distributions-a review," *Proc. IEEE*, vol. 77, no. 7, pp. 941–981, Jul. 1989.

[11] L. Durak and O. Arikan, "Short-time Fourier transform: Two fundamental properties and an optimal implementation," *IEEE Trans. Signal Process.*, vol. 51, no. 5, pp. 1231–1242, May 2003.

[12] M. A. Wieczorek and F. J. Simons, "Minimum variance multitaper spectral estimation on the sphere," *J. Fourier Anal. Appl.*, no. 6, pp. 665–692, 2008.

[13] F. Dahlen and F. J. Simons, "Spectral estimation on a sphere in geophysics an cosmology," *Geophys. J. Int.*, vol. 174, pp. 774–807, 2008.

[14] B. T. T. Yeo, W. Ou, and P. Golland, "On the construction of invertible filter banks on the 2-sphere," *IEEE Trans. Image Process.*, vol. 17, no. 3, pp. 283–300, Mar. 2008.

[15] J. R. Driscoll and D. M. Healy, "Computing Fourier transforms and convolutions on the 2-sphere," *Adv. Appl. Math.*, vol. 15, no. 2, pp. 202–250, Jun. 1994.

[16] W. Freeden and V. Michel, "Constructive approximation and numerical methods in geodetic research today. An attempt at a categorization based on an uncertainty principle," *J. Geodesy.*, vol. 73, pp. 452–465, 1999.

[17] F. J. Harris, "On the use of windows for harmonic analysis with the discrete Fourier transform," *Proc. IEEE*, vol. 66, no. 1, pp. 51–83, Jan. 1978.

[18] F. K. Hansen, K. M. Gorski, and E. Hivon, "Gabor transforms on the sphere with applications to CMB power spectrum estimation," *Mon. Not. R. Astron. Soc.*, vol. 336, no. 4, pp. 1304–1328, Nov. 2002.

[19] F. J. Simons, F. A. Dahlen, and M. A. Wieczorek, "Spatiospectral concentration on a sphere," *SIAM Rev.*, vol. 48, no. 3, pp. 504–536, 2006.